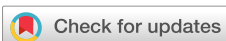


RESEARCH ARTICLE | SEPTEMBER 15 1976

## Observation of large dc supercurrents at nonzero voltages in Josephson tunnel junctions

J. Niemeyer; V. Kose



*Appl. Phys. Lett.* 29, 380–382 (1976)  
<https://doi.org/10.1063/1.89094>



### Articles You May Be Interested In

Anisotropic self-field effect in a-axis  $\text{YBa}_2\text{Cu}_3\text{O}_{7-x}/\text{Ag}/\text{PbIn}$  Josephson junctions

*Appl. Phys. Lett.* (March 1996)

Type II Superconductivity Experiment

*American Journal of Physics* (February 1968)

BaFe 1.8 Co 0.2 As 2 thin film hybrid Josephson junctions

*Appl. Phys. Lett.* (October 2010)

# Observation of large dc supercurrents at nonzero voltages in Josephson tunnel junctions

J. Niemeyer and V. Kose

Physikalisch-Technische Bundesanstalt, Braunschweig, West Germany  
(Received 5 April 1976; in final form 6 July 1976)

Large dc supercurrents at nonzero voltages are observed in dc current-biased small Josephson tunnel junctions of the type  $\text{PbIn}-(\text{PbIn})_x\text{O}_y-\text{Pb}$  with critical current densities  $j_0$  ranging from  $2 \times 10^2$  to  $2 \times 10^5 \text{ A/cm}^2$ . The dependence of the hysteresis on  $j_0$  and the form of the subharmonic energy gap structure are compared with the theoretical results of McDonald *et al.*

PACS numbers: 74.35.+x, 73.40.Rw

By analyzing a lumped circuit model of a dc current-biased Josephson junction, Stewart<sup>1</sup> und McCumber<sup>2</sup> independently explained why the observed dc current-voltage characteristic ( $I-\langle V \rangle$ ) differs for the various junction types [such as a superconductor-insulator-superconductor (SIS) thin-film junction, superconductor-normal metal-superconductor (SNS) junction, or point-contact junction, etc.]. They predicted that the dc supercurrent in the  $I-\langle V \rangle$  characteristic at nonzero voltages depends on the dimensionless quantity  $\beta_c = 2\pi C I_0 [R(I_0)]_s^2 / \phi_0$ , which includes only junction parameters, besides  $2\pi$  and the flux quantum  $\phi_0$ :  $C$ , the shunt capacity;  $[R(I_0)]_s$ , the phenomenological shunt resistance; and  $I_0$ , the critical dc supercurrent.  $\beta_c$  approaches infinity for low critical dc supercurrent density SIS junctions (light damping) and diminishes for SNS junctions (heavy damping). In the first case the dc supercurrent at nonzero voltages is minimal and large hysteresis occurs in the  $I-\langle V \rangle$  characteristic, whereas in the second case a maximum dc supercurrent with no hysteresis is obtained.

Recently, McDonald *et al.*<sup>3</sup> calculated the  $I-\langle V \rangle$  characteristic of a dc current-biased tunnel junction at  $T=0 \text{ K}$  by modifying Werthamer's tunneling theory.<sup>4</sup> By including the Mattis-Bardeen model<sup>5</sup> for the superconducting electrodes, they also showed the form of the subharmonic energy gap structure. Drastic changes in the  $I-\langle V \rangle$  characteristic are predicted, depending on the dimensionless parameter  $RC/\tau_\epsilon$ , where  $R$  is the junction normal state resistance,  $C$  the shunt capacity, and  $\tau_\epsilon = 2\phi_0/\langle V \rangle_\epsilon$ , with  $\langle V \rangle_\epsilon$  the gap voltage. However, the only experimental data presently available for comparison are from externally shunted tunnel junctions<sup>6,7</sup> and from tunnel junctions having small critical supercurrent densities  $j_0$ .<sup>8</sup>

We wish to present experimental results on  $I-\langle V \rangle$  characteristics of small SIS tunnel junctions of the type  $\text{PbIn}-(\text{PbIn})_x\text{O}_y-\text{Pb}$  over a wide range of  $j_0$  values. The mass content of In is 10%.<sup>9</sup> The magnetic field dependence of the dc supercurrent and the subharmonic energy gap structure is also displayed. The junctions were prepared by using the oblique evaporation method<sup>10</sup> and the insulating barrier was formed by thermal oxidation. The in-line junctions are lenticular in shape with areas ranging from  $100 \mu\text{m}^2$  at  $j_0 = 10^2 \text{ A/cm}^2$  to  $3 \mu\text{m}^2$  at  $j_0 = 10^5 \text{ A/cm}^2$ . The length of the junctions ranges from 6 to 1  $\mu\text{m}$ , respectively. To achieve an efficient heat transfer from the barrier, the adjacent

superconducting electrodes were 600 nm thick for the high-current-density junctions.

The dimensions of the junctions are small compared with all the relevant electromagnetic wavelengths such as that of the Josephson plasma frequency  $\omega_p/2\pi = (I_0/2\pi\mu_0 C)^{1/2}$ ,<sup>11</sup> or the gap frequency  $\nu_\epsilon = \langle V \rangle_\epsilon / \phi_0$ . Even at a current density of  $10^5 \text{ A/cm}^2$  the Josephson penetration depth  $\lambda_J = (\phi_0/2\pi\mu_0 j_0 d)^{1/2}$  is about twice the junction length where  $d$  incorporates the penetration depth of the superconductors and the thickness of the barrier.<sup>11</sup> Because the junction length is smaller than  $4\lambda_J$ , we exclude spatial variations of the supercurrent density across the junction area for zero magnetic field.<sup>12</sup> The experiments were carried out at a helium bath temperature of 4.2 K.

Figure 1 shows the influence of the critical dc supercurrent density  $j_0$  on the dc current-biased junctions. At increasing  $j_0$  the switching hysteresis characterized by  $I_R/I_0$  decreases. The reduced gap voltage at high current densities is caused by self-heating effects. The low-critical-current-density junction [see Fig. 1(a)] shows the subharmonic energy gap structure at voltages  $\langle V \rangle_m = \langle V \rangle_\epsilon/m$  with  $m = 2$  and  $m = 3$ , the beginning of the even  $m$  series probably caused by harmonics of the Josephson frequency, and the odd  $m$  series caused by processes of photon-assisted tunneling.<sup>13,14</sup> This structure has not been seen at higher current densities, which may also be expected from McDonald's results (see Ref. 3, Fig. 2), because due to the pair current, the total current comprising the large pair current and

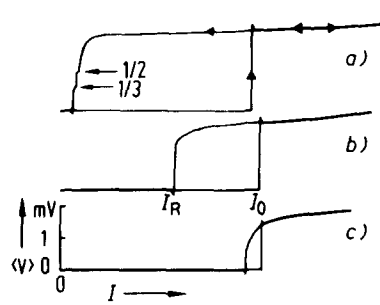


FIG. 1. Influence of the critical dc supercurrent density  $j_0$  on the  $I-\langle V \rangle$  characteristic of tunnel junctions. The hysteresis is characterized by the ratio of the reverse switching current  $I_R$  and the critical dc supercurrent  $I_0$ . Temperature  $T=4.2 \text{ K}$ . (a)  $j_0 = 3.1 \times 10^3 \text{ A/cm}^2$ ;  $I_0 = 0.68 \text{ mA}$ . (b)  $j_0 = 3.4 \times 10^4 \text{ A/cm}^2$ ;  $I_0 = 3.4 \text{ mA}$ . (c)  $j_0 = 2.1 \times 10^5 \text{ A/cm}^2$ ;  $I_0 = 6.4 \text{ mA}$ .

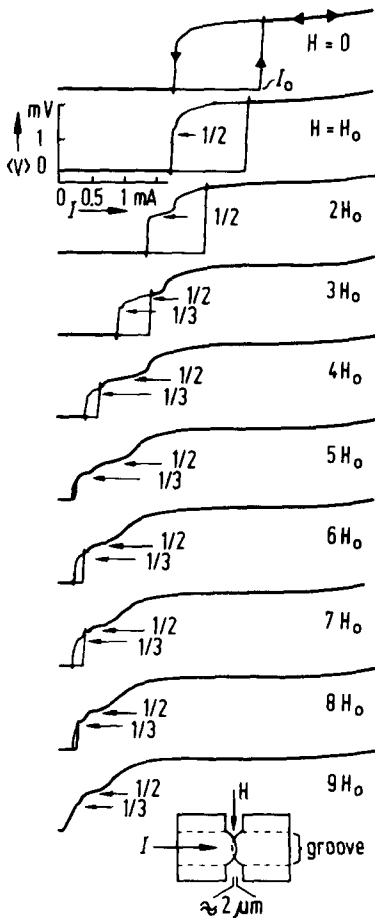


FIG. 2. Magnetic field dependence of the pair current of a tunnel junction.  $H_0 = 1, 2 \times 10^3$  A/m;  $j_0 = 3.4 \times 10^4$  A/cm<sup>2</sup>.

the quasiparticle current shows the lowest minimum in the  $I-\langle V \rangle$  characteristic at nonzero voltages between  $\langle V \rangle_m = \frac{1}{2}\langle V \rangle_\epsilon$  and gap voltage  $\langle V \rangle_\epsilon$ . Only when the pair current is suppressed by means of a magnetic field does the positive slope  $dI/d\langle V \rangle$  of the quasiparticle current appear in the  $I-\langle V \rangle$  characteristic and the subharmonic energy gap structure become visible (see Fig. 2). The magnetic field at about  $H = 5H_0$  corresponds to an absorption of one flux quantum in the junction.

Figure 3 shows the experimentally obtained relationship between the dc pair current density  $j_0$  over 3 orders of magnitude and the hysteresis parameter  $I_R/I_0$ . The solid line represents the experimental results (dots). The dashed curve (a) in Fig. 3 is obtained from the theory of McDonald *et al.*,<sup>3</sup> which is valid for  $T = 0$  K. The dimensionless parameter  $RC/\tau_\epsilon = \pi\epsilon'\epsilon_0 f \langle V \rangle_\epsilon^2 / 8\phi_0 t j_0$  is obtained by introducing  $\tau_\epsilon = 2\phi_0/\langle V \rangle_\epsilon$ ,  $I_0 R = \frac{1}{4}\pi\langle V \rangle_\epsilon f$ , where we assumed  $f$  to be 0.788 due to the strong coupling of the superconductors used,<sup>15,16</sup>  $\epsilon_0$  is the permittivity of vacuum.

In spite of the rough assumptions, relative permittivity  $\epsilon' = 8$  and barrier thickness  $t = 2$  nm,<sup>17</sup> which can be different for the PbIn alloy, and the fact that the theory is only valid for zero temperature, the experimental data agree qualitatively with the theory of Ref. 3. For the temperature dependence of the gap voltage we used the measured value  $\langle V \rangle_\epsilon = 2.2$  mV. We think

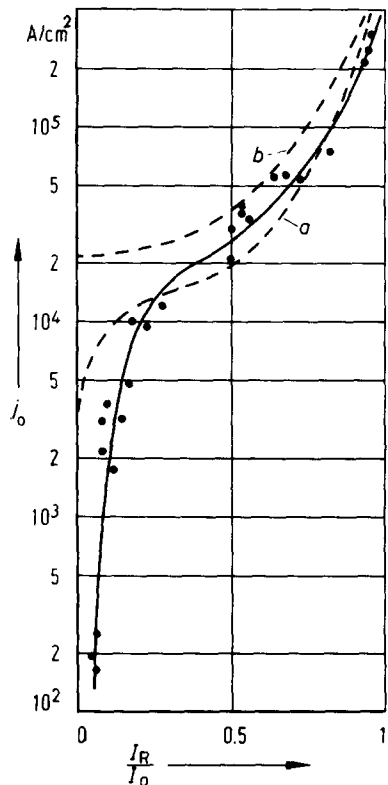


FIG. 3. Critical pair-current density  $j_0$  vs hysteresis parameter  $I_R/I_0$  of small PbIn-(PbIn)<sub>x</sub>O<sub>y</sub>-Pb thin-film tunnel junctions at  $T = 4.2$  K. Solid line represents the experimental data (see dots). (a) Theoretical result from McDonald *et al.* valid for  $T = 0$  K. (b) Theoretical result from Stewart (nonlinear shunt resistance).

that the deviations, especially at low current densities, can possibly be explained by the temperature dependence of the quasiparticle current and the pair current at nonzero voltages.<sup>18</sup> There is also the influence of the quasiparticle-pair interference term on the hysteresis.<sup>19</sup> Stewart<sup>18</sup> has analyzed a lumped circuit model using a nonlinear shunt resistance, which means strong idealization of the zero-temperature tunneling characteristic [see Fig. 3(b)]. His dimensionless parameter  $k_{n..} = \phi_0 J_0 / 2\pi C \langle V \rangle_\epsilon^2$  is used, which is directly related to  $RC/\tau_\epsilon$  by  $1/k_{n..} = (16/f) RC/\tau_\epsilon$ . One should take note of the fact that no attempts were made to introduce  $f$  in his theory.

The authors wish to acknowledge stimulating and useful discussions with D.G. McDonald and R.E. Harris and are indebted to D.G. McDonald for providing his theoretical results prior to publication.

<sup>1</sup>W.C. Stewart, Appl. Phys. Lett. 12, 277 (1968).

<sup>2</sup>D.E. McCumber, J. Appl. Phys. 39, 3113 (1968).

<sup>3</sup>D.G. McDonald, E.G. Johnson, and R.E. Harris, Phys. Rev. B 13, 1028 (1976).

<sup>4</sup>N.R. Werthamer, Phys. Rev. 147, 255 (1966).

<sup>5</sup>D.C. Mattis and J. Bardeen, Phys. Rev. 111, 412 (1958).

<sup>6</sup>P.K. Hansma and G.I. Roohlin, J. Appl. Phys. 43, 4721 (1972).

<sup>7</sup>T.A. Fulton, Phys. Rev. B 7, 1189 (1973).

<sup>8</sup>W.C. Scott, Appl. Phys. Lett. 17, 166 (1970).

- <sup>9</sup>A. Emmanuel, G. B. Donaldson, W. T. Band, and D. Dew-Hughes, IEEE Trans. Magn. MAG-11, 763 (1975).
- <sup>10</sup>J. Niemeyer, PTB-Mitt. 84, 251 (1974).
- <sup>11</sup>B. D. Josephson, Adv. Phys. 14, 419 (1965).
- <sup>12</sup>W. J. Johnson and A. Barone, J. Appl. Phys. 41, 2958 (1970).
- <sup>13</sup>L. E. Hasselberg, M. T. Levinsen, and M. R. Samuels, Phys. Rev. B 9, 3757 (1974).
- <sup>14</sup>B. N. Taylor and E. Burstein, Phys. Rev. Lett. 10, 14 (1963).
- <sup>15</sup>V. Ambegaokar and A. Baratoff, Phys. Rev. Lett. 10, 486 (1963); 11, 104 (E) (1963).
- <sup>16</sup>T. A. Fulton and D. E. McCumber, Phys. Rev. 175, 585 (1968).
- <sup>17</sup>S. Basavaiah, J. M. Eldridge, and J. Matisoo, J. Appl. Phys. 45, 457 (1974).
- <sup>18</sup>W. C. Stewart, J. Appl. Phys. 45, 452 (1974).
- <sup>19</sup>F. Auracher, P. L. Richards, and G. I. Rochlin, Phys. Rev. B 8, 4182 (1973).

## Thermomechanical heat generation in copper and a Nb-Ti superconducting composite\*

D. S. Easton and D. M. Kroeger

Metals and Ceramics Division, Oak Ridge National Laboratory, Oak Ridge, Tennessee 37830

A. Moazed

University of Tennessee, Knoxville, Tennessee 37916

(Received 17 May 1976; in final form 6 July 1976)

Heat generation via tensile stresses in both pure copper and a superconducting Nb-Ti composite was studied at 300 and 4.2 K. Linear thermoelastic behavior was found at room temperature but not at 4.2 K. At 4.2 K, stress levels on the order of 88 MPa and 0.1% strain produced energy losses of  $1 \text{ to } 2 \times 10^5 \text{ J/m}^3$ . When stress cycled under adiabatic conditions, the composite showed a temperature increase with each cycle as a result of nonlinear (hysteretic) stress/strain behavior.

PACS numbers: 74.20.-z, 65.70.+y, 81.45.+r, 62.40.+i

Recent experiments,<sup>1-5</sup> in which hysteresis loops found in the stress-strain curves of Nb-Ti composites, indicated that large temperature increases might be associated with these loops. This work establishes the production of heat in Nb-Ti composites when subjected to tensile stress/strain and shows that large temperature rises will occur unless the material is adequately cooled.

An annealed pure copper sample and a commercially produced superconducting composite containing 18 filaments (0.25-mm diameter) of Nb-48 wt% Ti in a Cu matrix (Cu/Nb-Ti ratio of 2.7) were studied. Both samples had  $\sim 4.2 \text{ mm}^2$  cross-sectional area. The samples were thermally isolated in a vacuum environment to create nearly adiabatic conditions as shown in Fig. 1.

This apparatus was installed in a 4.2 K cryostat incorporating a 10 000 lb Instron tensile machine. A description of this equipment along with stress/strain curves of materials used in this work has been reported earlier.<sup>1/2</sup> The tensile force necessary to overcome atmospheric pressure on the bellows was measured and corrected. Thermal decay curves show that heat loss from the sample to the helium bath is negligible through the micarta pull rods. Cryopumping by the 4.2 K walls along with the use of an oil diffusion pump produces very low pressures within the chamber. In a totally evacuated condition, the system required an excessively long time to recover from any heat injection; therefore, in most cases a small amount of helium gas was introduced to improve heat transfer to the helium bath. Chromel-constantan and Chromel P versus gold-0.07%

Fe thermocouples were used for temperature measurements at 300 and 4.2 K, respectively. A 2-pen X-Y recorder monitored load and temperature versus time.

At room temperature, the linear thermoelastic effect is dominant. A temperature decrease directly proportional to the tensile stress occurred upon the application of load and an identical temperature rise accompanied unloading. No thermoelastic cooling was re-

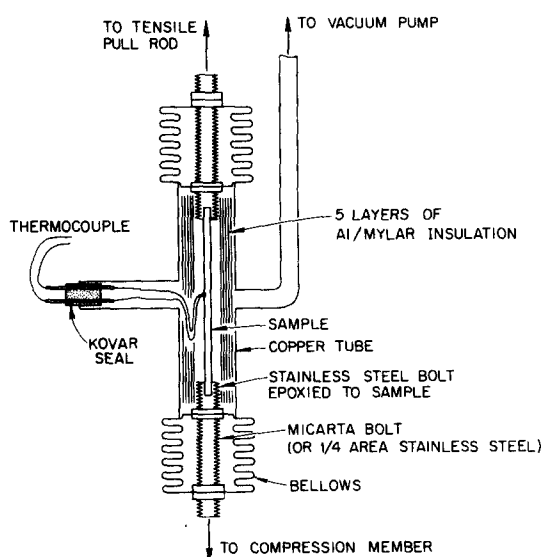


FIG. 1. Apparatus for measuring strain-induced heat generation.